

NUMERICAL ANALYSIS OF REINFORCED CONCRETE BEAM-COLUMN JOINT UNDER ACCIDENTAL IMPACT

Sergey Savin

Department of Reinforced Concrete and Masonry Structures, Moscow State University of Civil Engineering, Moscow, Russian Federation
e-mail: suwin@yandex.ru

Abstract

The purpose of this study is to build a universal computational model of a plane-stressed joint element, which could be implemented as a special finite element of the interface node and integrated into the standard finite element analysis procedure to improve the accuracy of its results when assessing the structural behavior of 2D stressed frame nodes. In order to simulate the force resistance of monolithic reinforced concrete units of building frames, the article uses a combination of the finite element method and the finite difference method. The finite difference method is used directly to study the stress-strain state of a plane stressed element of a monolithic joint, and the FEM is used to obtain the boundary conditions of the problem. A distinctive feature of the proposed model is the ability to take into account the discrete nature of the reinforcement, as well as the violation of the adhesion of the reinforcement to concrete along the contact surface. For the purposes of implementing the model, an algorithm for calculating the stress-strain state of the beam-column joint is proposed. An example of calculating an experimental frame unit based on the proposed approach is considered.

Keywords: finite difference method, reinforced concrete, beam-column joint, plane stress state, progressive collapse

1. Introduction

When assessing the resistance of reinforced concrete frame-tie frames of buildings and structures to progressive collapse, taking into account the possibility of local destruction in them, in any section of the bearing system, researchers and design engineers mainly use a spatial rod, plate, or plate-rod finite element (FE) models such as considered by Gudmundsson and Izzuddin (2010), Izzuddin et al. (2008), Kolchunov et al. (2019); Kolchunov and Savin (2018), Li et al. (2016), Marjanishvili and Agnew (2006), Shan, Petrone and Kunnath (2019), Wang et al. (2014) or similar models of the Applied Element Method investigated by Alanani, Ehab and Salem (2020), Tagel-Din and Meguro (2000). For a more detailed analysis of the features of deformation and the destruction of nodal joints, substructures, fragments of frames of buildings and structures under special influences caused by structural rearrangements of their bearing systems due to the sudden removal of one of the elements, using the decomposition method, such elements are separated from the spatial design model of the entire structure. A computational analysis of their 3D or 2D finite element models is performed after the separation, as it was carried out by

Fedorova and Vu (2019), Kai and Li (2012); Sasani, Werner and Kazemi (2011), Yu, Luo and Li (2018).

The results of such numerical modeling, in combination with the data of experimental studies, demonstrated the need to take into account the peculiarities of the operation of nodal connections of load-bearing structures, such as beam-column, slab-column, etc., to ensure overall resistance to the progressive collapse of the load-bearing systems of buildings and structures. In the listed types of nodal connections and sections of bar structures (beams, columns), directly adjacent to such nodes, a biaxial or volumetric stress state is realized, which requires taking into account additional components of stresses and deformations. In this regard, for a more accurate evaluation of the stress-strain state of the bearing structures under loads, it is advisable to combine two approaches listed above: finite element analysis of spatial bar models and advanced analysis of nodal joint simulated by 3D finite elements or assessment based on simplified semi-empirical models.

The combination of such approaches in addition to taking into account the variation of scenarios of design load combinations leads to a high laboriousness of solving the problem under consideration. In this regard, high requirements are imposed on the qualifications of the designer-constructor, who, on the one hand, must be able to correctly select the most unfavorable scenarios of possible impacts, and on the other hand, exclude minor variants, obviously not posing a threat to the structural safety of the structure. However, even in this case, due to the presence of a human factor, one of the scenarios of an emergency design situation can slip out of sight, which can subsequently be realized during the life cycle of the structure. Therefore, to reduce the complexity of computations when enumerating a large number of possible variants of initial local fractures, computational models can be used, which, by analogy with the method of applied elements, would consist of bar elements of columns and beams interconnected by elastic-yielding bonds. The parameters of such bonds would be refined by solving a plane or volumetric problem of the nonlinear theory of elasticity of an anisotropic body. Analysis of the calculated models of the beam-column joints presented in the scientific literature shows that most of them are based on a simplified representation of a 3D or 2D stressed element by replacing stresses with generalized forces. Thus, highlighting two characteristic resistance mechanisms, truss and compressed inclined strip, Hwang and Lee (2000) evaluate the possibility of their implementation separately. A similar approach to the analysis of the operation of the girder and column interface nodes, which are slightly different in their design, can be found in the works of Hayati and Hamid (2015), Tsonos (2008); Yu and Tan (2013). Ahmadi et al. (2016), Feng et al. (2019), Feng, Wu and Lu (2018) modeled the structural behavior of a flat joint element using elastic ties (springs). The introduction of such elastic-yielding springs between elements into the design model allowed Feng et al. (2019) to achieve better quantitative and qualitative convergence with experimental data than the traditional bar models of the finite element method with rigid nodal connections. However, this approach does not allow assessing the resistance of the nodal joint separately.

When investigating a 2D fragment of a multi-story building frame, Fedorova, Vu Ngoc Tuyen, and Yakovenko (2020) applied a shell FE model to assess the structural behavior of the beam-column nodal joint. They performed strength analysis of nodal joint on the bases of yield surface of concrete under two-dimensional stress-strain state suggested by Geniyev, Kisyuk, and Tyupin (1974). The use of strength criterion according to the yield surface in combination with the use of shell FE models of 2D stressed nodal joint leads to time-consuming computations when we describe a large number of impact scenarios. At the same time, it seems that the approach to strength assessment applied by Fedorova, Vu Ngoc Tuyen, Yakovenko (2020) is quite effective and can be supplemented with a model of a special element that simulates a nodal joint. Such an element could be integrated into the spatial bar and plate-bar FE computational models to improve their accuracy.

Summarizing the results of approaches for structural behavior simulation of buildings and structures, taking into account the peculiarities of deformation and destruction of their beam-column nodal joints, it can be concluded the absence of simplified design models which allow evaluation of strength, both of bar member and 2D and 3D, stressed nodal joints of this bar members during unified calculation procedure. In this regard, the purpose of this study is the construction of a 2D stressed nodal joint computational model that could be implemented into the standard procedure of finite element analysis as a special finite element to improve the accuracy of structural analysis.

2. Models and methods

2.1 Strength criteria for composite 2D stressed structural member

In order to assess the deformation and destruction of nodal joints of the reinforced concrete frame, as presented in Figure 1a, in this study we used a model of a load-bearing system consisting of universal physically nonlinear bar finite elements of beams and columns and special elements which simulate the joint presented in Figure 1b and Figure 1c. In this case, the stress-strain states of the sections at the ends of the bar members are the boundary conditions for calculating the node. Further, the solution to the problem of estimating the stress state of a node is carried out in the plane stresses formulation, neglecting the stresses out of the plane of the load action. We suppose that they are small in comparison with the stresses acting in the plane. In this paper, the contour of the reinforced concrete beam-column joint has a rectangular form as it is shown in Figure 1d. However, it should be noted that boundaries of the 2D stressed zone spread on the parts of beams and columns adjacent to the node. Therefore, T, Γ and + shaped nodes should be considered for a more accurate assessment of joint stress-strain state.

In contrast to the traditional approaches that use super elements, in this study, the general solution to the problem of the plane stress state of a monolithic beam-column nodal joint is based on the finite differences' method in displacements' form. The usage of the finite-difference method allows us to construct a simplified algorithm for assessing the convergence of the calculation results and adjusting the density of the region partitioning to achieve the required accuracy. Also, it provides the ability to take into account cracks' formation and drift between reinforcement bars and concrete matrix. On the other hand, the displacements' formulation to the problem makes it possible to avoid searching for stress function on the contour of the joint area.

To assess the strength of a monolithic beam-column joint under design load action, we apply the strength condition for a plane-stressed concrete member, which following the theory of concrete plasticity proposed by Geniyev, Kisyuk and Tyupin (1974) can be written as follows:

$$\sigma_x^2 + \sigma_y^2 - \sigma_x \sigma_y + 3\tau_{xy}^2 - (R_c - R_t)(\sigma_x - \sigma_y) \leq R_c R_t, \quad (1)$$

where σ_x , σ_y , τ_{xy} are normal and tangent stresses acting along with the faces of an elementary parallelepiped outlined in the vicinity of a certain point of the beam-column joint; R_c , R_t are the standard ultimate strength of concrete under uniaxial compression and tension respectively.

The graphical interpretation of inequality (1) is an ellipse displayed in the coordinate axes of the principal stresses $\sigma_1 - \sigma_2$. The strength of the elementary volume of the beam-column nodal joint under consideration is ensured when the point corresponding to the current stress-strain state lies inside the ellipse described by inequality (1).

Here, condition (1) is written for concrete, since the distance between the reinforcing bars at the beam-column joint of the reinforced concrete frame is comparable to the dimensions of the nodal joint itself. In this regard, the usage of the strength condition for reinforced concrete when

the reinforcement is "smeared" over the entire element, can lead to unjustified errors. Therefore, when constructing a general solution, we assume that at the nodes intersected by the reinforcing bars, the material is structurally orthotropic with the given deformability parameters, and at other mesh nodes, it is isotropic if the strength condition (1) is satisfied.

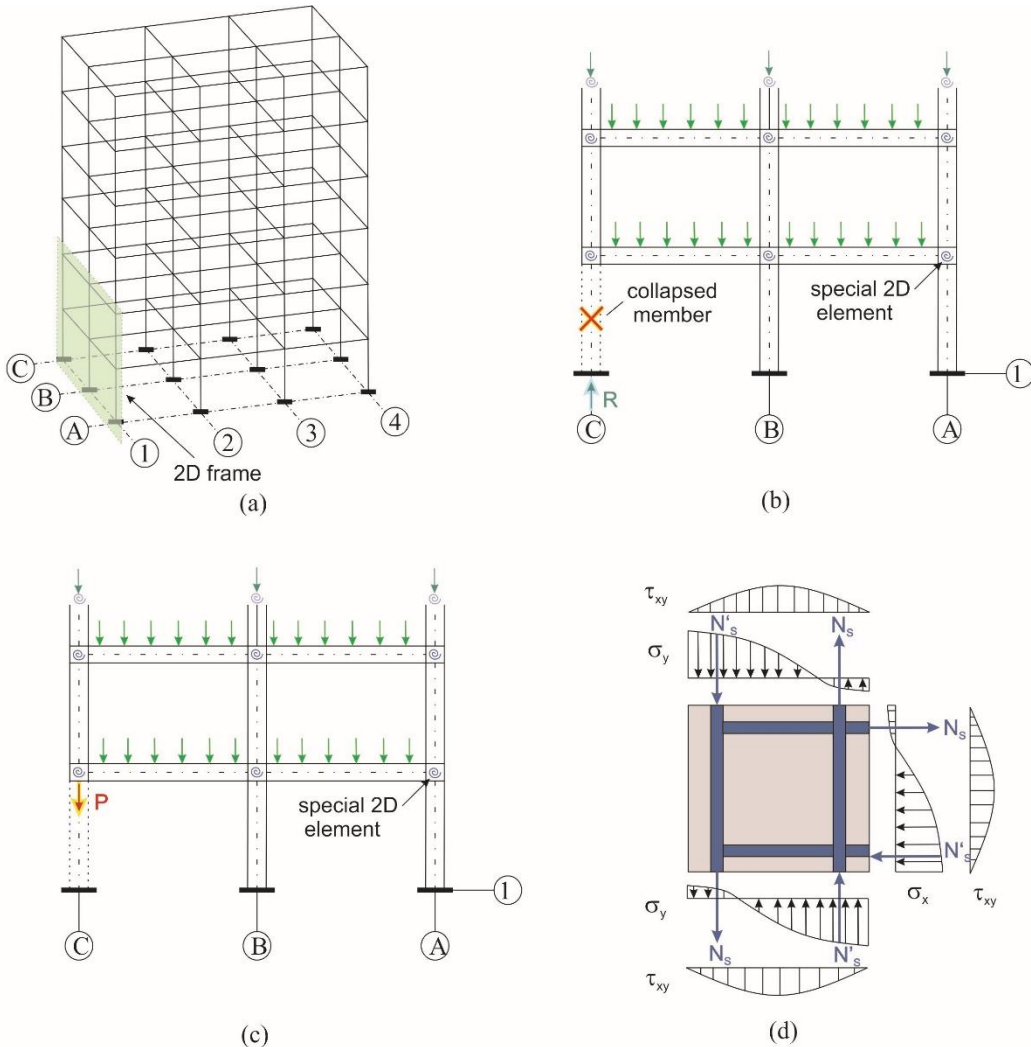


Fig. 1. Design schemes of a reinforced concrete frame. (a) Spatial bar model of the entire building frame; (b) Primary computational model of a 2D fragment of the frame in the area of expected accidental impact; (c) Secondary computational model of a 2D fragment of the frame under accidental impact; (d) Beam-column joint model.

2.2 Equilibrium equations of the finite-difference method for 2D stressed composite nodal joint

In accordance with the two-dimensional formulation of the problem, the equilibrium equations for an infinitesimal volume of an orthotropic body can be written in displacements as follows:

$$\begin{aligned} \frac{E_x}{1-\mu^2} \frac{\partial^2 u}{\partial x^2} + \frac{E_y \mu_x}{1-\mu^2} \frac{\partial^2 v}{\partial x \partial y} + G_{xy} \left(\frac{\partial^2 u}{\partial y^2} + \frac{\partial^2 v}{\partial x \partial y} \right) &= 0; \\ \frac{E_y}{1-\mu^2} \frac{\partial^2 v}{\partial y^2} + \frac{E_x \mu_y}{1-\mu^2} \frac{\partial^2 u}{\partial x \partial y} + G_{xy} \left(\frac{\partial^2 v}{\partial x^2} + \frac{\partial^2 u}{\partial x \partial y} \right) &= 0, \end{aligned} \quad (2)$$

where u , v are displacements of grid nodes along the orthogonal coordinate axes X and Y , respectively;

E_x , E_y are reduced elasticity moduli of material along orthogonal coordinate axes X and Y , respectively;

μ is Poisson's ratio, taken as for concrete $\mu = 0.2$;

$$G_{xy} = 2\sqrt{E_x E_y} / (1+\nu); \quad \mu_x = \mu\sqrt{E_x/E_y}; \quad \mu_y = \mu\sqrt{E_y/E_x}. \quad (3)$$

In equations (2), we neglected the components of the volumetric forces from the self-weight of the material, since they do not make a significant contribution to the general stress state of the element at the loading stages under consideration.

We divide the area of the joint by a grid with the same horizontal and vertical spacing so that the centers of gravity of the reinforcing bars coincide with the grid lines as Figure 2a shows.

Let us write down the derivatives in the equations (2) in the finite-differences taking into account the rule of numbering grid nodes in Figure 2b:

$$\begin{aligned} \frac{\partial^2 u_i}{\partial x^2} &= \frac{u_{(i-1)} - 2u_i + u_{(i+1)}}{\Delta^2}; \quad \frac{\partial^2 v_i}{\partial y^2} = \frac{v_{(i-n-1)} - 2v_i + v_{(i+n+1)}}{\Delta^2}; \\ \frac{\partial^2 u_i}{\partial y^2} &= \frac{u_{(i-n-1)} - 2u_i + u_{(i+n+1)}}{\Delta^2}; \quad \frac{\partial^2 v_i}{\partial x^2} = \frac{v_{(i-1)} - 2v_i + v_{(i+1)}}{\Delta^2}; \\ \frac{\partial^2 u_i}{\partial x \partial y} &= \frac{u_{(i-n)} - u_{(i-n-2)} + u_{(i+n+2)} - u_{(i+n)}}{4\Delta^2}; \\ \frac{\partial^2 v_i}{\partial x \partial y} &= \frac{v_{(i-n-2)} - v_{(i+n)} + v_{(i-n)} - v_{(i+n+2)}}{4\Delta^2}, \end{aligned} \quad (4)$$

where Δ is the step of the grid lines in accordance with Figure 2b.

For the mixed derivative, we additionally write an expression in one-sided differences, which will allow us to relate the equilibrium equations (2) for the corner points of the contour of the element under consideration to the boundary conditions:

$$\begin{aligned} \frac{\partial^2 u_i}{\partial x \partial y} &= \frac{u_{(i-n)} - u_{(i-n-1)} + u_{(i+n+2)} - u_{(i+n+1)}}{\Delta^2} = \frac{u_{(i-n-1)} - u_{(i-n-2)} + u_{(i+n+1)} - u_{(i+n)}}{\Delta^2}; \\ \frac{\partial^2 v_i}{\partial x \partial y} &= \frac{v_{(i-n-2)} - v_{(i-1)} + v_{(i-n)} - v_{(i+1)}}{\Delta^2} = \frac{v_{(i-1)} - v_{(i+n)} + v_{(i+1)} - v_{(i+n+2)}}{\Delta^2}. \end{aligned} \quad (5)$$

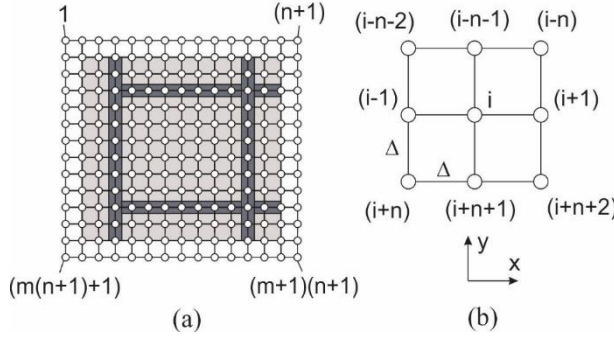


Fig. 2. Scheme for the calculation of a joint element using the finite-difference method.
(a) General view; (b) Accepted rule of numbering grid nodes.

Then equations (2) for the i -th point of the considered plane stressed element excepting corner points and taking into account (4) can be rewritten as:

$$4\left(a_{(i-1)}u_{(i-1)} - 2a_{(i+1)}u_{(i+1)} + a_{(i+1)}u_{(i+1)}\right) + \left(b_{(i-n-2)}v_{(i-n-2)} - b_{(i+n)}v_{(i+n)} + b_{(i-n)}v_{(i-n)} - b_{(i+n+2)}v_{(i+n+2)}\right) + \left(4d_{(i-n-1)}u_{(i-n-1)} - 8d_i u_i + 4d_{(i+n+1)}u_{(i+n+1)} + d_{(i-n-2)}v_{(i-n-2)} - d_{(i+n)}v_{(i+n)} + d_{(i-n)}v_{(i-n)} - d_{(i+n+2)}v_{(i+n+2)}\right) = 0; \quad (6)$$

$$4\left(c_{(i-n-1)}v_{(i-n-1)} - 2c_i v_i + c_{(i+n+1)}v_{(i+n+1)}\right) + \left(b_{(i-n)}u_{(i-n)} - b_{(i-n-2)}u_{(i-n-2)} + b_{(i+n+2)}u_{(i+n+2)} - b_{(i+n)}u_{(i+n)}\right) + \left(4d_{(i-1)}v_{(i-1)} - 8d_i v_i + 4d_{(i+1)}v_{(i+1)} + d_{(i-n)}u_{(i-n)} - d_{(i-n-2)}u_{(i-n-2)} + d_{(i+n+2)}u_{(i+n+2)} - d_{(i+n)}u_{(i+n)}\right) = 0.$$

For the corner points of the contour, expressions (5) should be substituted into equations (2) instead of expressions (4).

When deriving equations (6), the following designations that were adopted: a_i , b_i , c_i , d_i are the coefficients of reduction of the deformability parameters of materials at the nodes intersected by the reinforcing bars, as well as the arbitrary nodes of the element under consideration in the deformed state and determined from the relations:

$$a_i = \frac{E_{x,i}}{1-\mu^2} = \frac{E_c + kE_s \frac{A_{sx}}{b_{col}\Delta}}{1-\mu^2}; \quad c_i = \frac{E_{y,i}}{1-\mu^2} = \frac{E_c + kE_s \frac{A_{sy}}{b_{col}\Delta}}{1-\mu^2};$$

$$b_i = \frac{E_{x,i}\mu_{y,i}}{1-\mu^2} = \frac{E_{y,i}\mu_{x,i}}{1-\mu^2} = \frac{E_c + kE_s \frac{A_{sx}}{b_{col}\Delta}}{1-\mu^2} \mu_{y,i} = \frac{E_c + kE_s \frac{A_{sy}}{b_{col}\Delta}}{1-\mu^2} \mu_{x,i}; \quad (7)$$

$$d_i = G_{xy,i} = \frac{E_c}{2(1+\mu)} \sqrt{\left(1 + k \frac{E_s}{E_c} \frac{A_{sx}}{b_{col}\Delta}\right) \left(1 + k \frac{E_s}{E_c} \frac{A_{sy}}{b_{col}\Delta}\right)},$$

where E_c , E_s are secant elasticity moduli of concrete and reinforcement, respectively.

A_{sx} , A_{sy} are a cross-sectional area of reinforcing bars along the X and Y axes, respectively, which axes pass through the i -th grid node;

b_{col} is the column cross-sectional width;

Δ is the step of the grid lines dividing the area of the considered joint;

k is a coefficient that takes into account the drift between reinforcement bars and concrete due to shear forces' action. This coefficient takes the value in the range from 0 to 1, where 1 corresponds to the complete transfer of forces between reinforcement and concrete, and 0 corresponds to the complete absence of adhesion between the reinforcement and concrete.

2.3 Method for assessment the structural behavior of 2D beam-column joint of reinforced concrete frame

In order to algorithmize the solution of equations (6) in finite differences, we specify the rules for numbering points inside the area, on the contour of the area and beyond the contour of the area under consideration. In accordance with Figure 2, the following conditions will be met for points on the contour:

- for the top edge of the contour: $i \in [n + 3, 2n + 1]$;
- for the bottom edge of the contour: $i \in [(n + 1)(m - 1) + 2, (n + 1)(m - 1) + n]$;
- for the left edge of the contour: $i = (n + 3) + j(n + 1)$;
- for the right edge of the contour: $i = (2n + 1) + j(n + 1)$;
- corner points of the contour: $i = n + 3; 2n + 1; (n + 1)(m - 1) + 2; (n + 1)(m - 1) + n$.

The conditions for the location of the grid nodes behind the contour of the beam-column joint member under consideration is as follows:

- over the contour: $i \in [1, n + 1]$;
- under the contour: $i \in [(n + 1)m + 1, (n + 1)(m + 1)]$;
- to the left of the contour: $i = 1 + l(n + 1)$;
- to the right of the contour: $i = (n + 1)(l + 1)$.

Above, we adopted the following designations: n, m are respectively the number of horizontal and vertical steps of the grid, which split the joint member; $j = 0, 1, \dots, (m - 2)$; $l = 0, 1, \dots, m$.

Taking into account the accepted rules for the numbering of grid nodes, the algorithm for calculating the stress-strain state of the crossbar and column interface will consist of the following stages:

Stage 1. Construction of a spatial bar FE model, setting boundary conditions, stiffnesses, loads, and actions.

Stage 2. Structural analysis of the frame for the design combination of loads; determination of the deformed state of the bars adjacent to the monolithic beam-column joint.

Stage 3. Dividing the area of the beam-column joint with a grid of nodes, drawing up the equations of the grid method in matrix form:

$$K \cdot q + P = 0, \quad (8)$$

where K is the matrix of coefficients for unknown displacements u_i, v_i of the system of equations (6) or, in other words, stiffness matrix;

q is the vector of the unknown displacements u_i, v_i from the equations (6);

P is the load vector or the vector of the free terms of the equations (6).

As the boundary conditions for solving equations (8), the values of stresses σ_x , σ_y , τ_{xy} at the corresponding points of the contour calculated at stage 2 are used:

$$\begin{aligned}\sigma_{x,i} &= \frac{1}{2\Delta(1-\mu^2)} \left[E_{x,i} (u_{(i+1)} - u_{(i-1)}) + E_{y,i} \mu_{x,i} (v_{(i-n-1)} - v_{(i+n+1)}) \right], \\ \sigma_{y,i} &= \frac{1}{2\Delta(1-\mu^2)} \left[E_{y,i} (v_{(i-n-1)} - v_{(i+n+1)}) + E_{x,i} \mu_{y,i} (u_{(i+1)} - u_{(i-1)}) \right], \\ \tau_{xy,i} &= \frac{G_{xy}}{2\Delta} (u_{(i-n-1)} - u_{(i+n+1)} + v_{(i+1)} - v_{(i-1)}).\end{aligned}\quad (9)$$

Stage 4. Calculation of the stress-strain state of the beam-column joint according to (8), (9) with the grid density n , m at the first iteration and $2n$, $2m$ at the second iteration. Assessing the convergence of the first and second iteration results. If the discrepancy between the stress-strain state parameters for a given partition density for the first and second iterations exceeds the required accuracy, then the mesh of nodes is refined until the difference in the calculation results for two successive iterations is within acceptable limits.

Stage 5. Refinement of the deformed state of the entire frame, taking into account the obtained calculation results for stage 4. If there are discrepancies in the parameters of the stress-strain state of the bar cross-sections adjacent to the beam-column joint, then we return to stage 4 and recalculate the stress-strain state of the beam-column joint until the required accuracy is achieved.

Stage 6. Calculation of a reinforced concrete frame for an accidental impact caused by the sudden removal of one of the structural members. The sequence of calculation is similar to steps 2-5.

Stage 7. Checking the strength criterion (1) for the beam-column joint at all grid nodes. If according to the results of the calculation, the strength condition is violated at any node of the mesh, then this one is considered as lying on the interior contour of the region when performing subsequent calculations.

2.4 Implementation of the proposed special element into FEA procedure

In the Eq. (8), the matrix K is an analogue of the FE stiffness matrix presented in the manual book by Gorodetskiy A. et al. (2019). The load vector P can be calculated based on the force boundary conditions on the contour of the 2D stressed beam-to-column joint presented in Fig. 1d. In this case, the equilibrium conditions should be satisfied for the components of the forces in the nodes of the 2D stressed joint and the nodes of the bar FE of the columns and beams adjacent to it. This study focuses on the 2D problem only. Therefore, the bar FE nodes have three degrees of freedom X , Z , U_y : two linear displacements and rotation about the Y axis. However, the nodes of the 2D 'beam-column' joint have only 2 degrees of freedom: X , Z . The rotational degree of freedom of nodes of the 2D joint is replaced by the introduction of a perfectly rigid body including the end node of the bar FE as a principal node. The perfectly rigid body nodes have been linked with nodes of the 2D stressed joint by connectors (spring FE) for linear and shear deformation transmission. A scheme of such a connection is shown in Figure 3.

During the calculation, the deformations are determined along with the depth of the beam or column cross-section at the end nodes adjacent to the 2D joint. Using the stress-strain relationship $\sigma = f(\epsilon)$, we find the components of normal stresses in the contour nodes of a special joint element. Shear stresses are determined based on the formula of D. Zhuravsky:

$$\tau = \frac{V \cdot S_{red}}{I_{red} \cdot d}, \quad (10)$$

where V is the shear force in the bar FE node adjacent to the 2D stressed beam-to-column joint;

S_{red} , I_{red} are static (first order) moment and moment of inertia (second order moment) of transformed cross section for the beam or column;

d is the cross-section depth in the frame plain.

Since the program code of the Lira-CAD software is closed, the analysis of the stress-strain state of a 2D stressed 'beam-column' joint was carried out in MathCAD Prime 4.0 based on the relations proposed in Sec. 2.3. For the calculation purpose, the parameters of the load vector P on the contour of the special element and the original FE model were refined using the obtained displacement vector q .

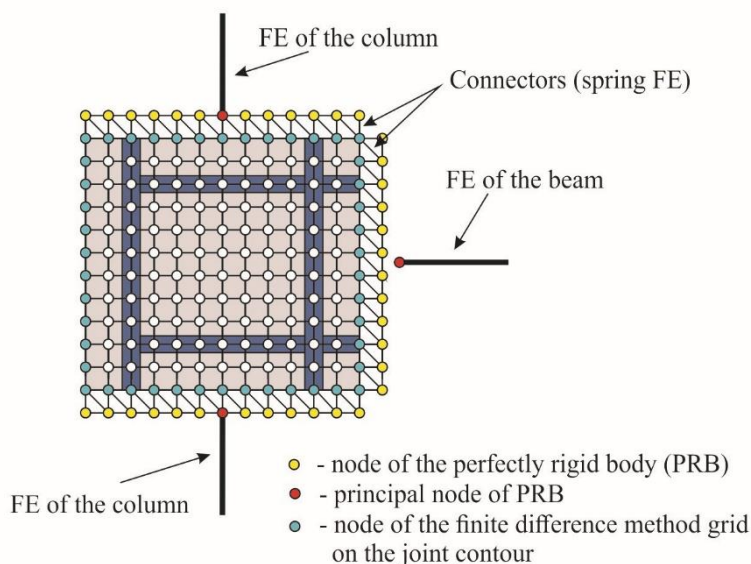


Fig. 3. Connection of the proposed 2D beam-to-column joint special element with bar FE.

3. Numerical simulation

3.1 Parameters of the test reinforced concrete frame and physical simulation of the accidental impact

For the purpose of the study of the stress-strain state of a 2D stressed joint "beam-column", the reinforced concrete frame considered by Savin, Kolchunov and Korenkov (2020) was chosen. Its reinforcement scheme and the general view is shown in Figure 4 (a,b) respectively. The materials of the frames were accepted in accordance with the Building Code of Russian Federation SP 63.13330.2018 (2019) as followed: concrete of compression strength class B25/ C_{20/25} (an equivalent designation is indicated after a slash in accordance with EN 1992-1-1 (2004)). The value of concrete prism compressive strength is $R_{b,n} = 18.5$ MPa (or characteristic compressive cylinder strength of concrete at 28 days $f_{ck} = 20$ MPa in accordance with EN 1992-1-1 (2004)), and the tangent modulus of elasticity is $E_{c(28)} = 30000$ MPa. The columns and girders are reinforced by spatial reinforcement cages with axial steel wire of class Bp500 (yield strength of

reinforcement $f_y = 500$ MPa, the value of modulus of elasticity of reinforcing steel $E_s = 200000$ MPa) and transverse reinforcing steel (stirrups) of class A300 (yield strength of reinforcement $f_y = 300$ MPa, the value of modulus of elasticity of reinforcing steel $E_s = 200000$ MPa). At the stage of normal operation, axial forces $P_1 = 4$ kN, $P_2 = 20$ kN, $P_3 = 16$ kN have been applied to the upper nodes of the frame as Figure 5a shows.

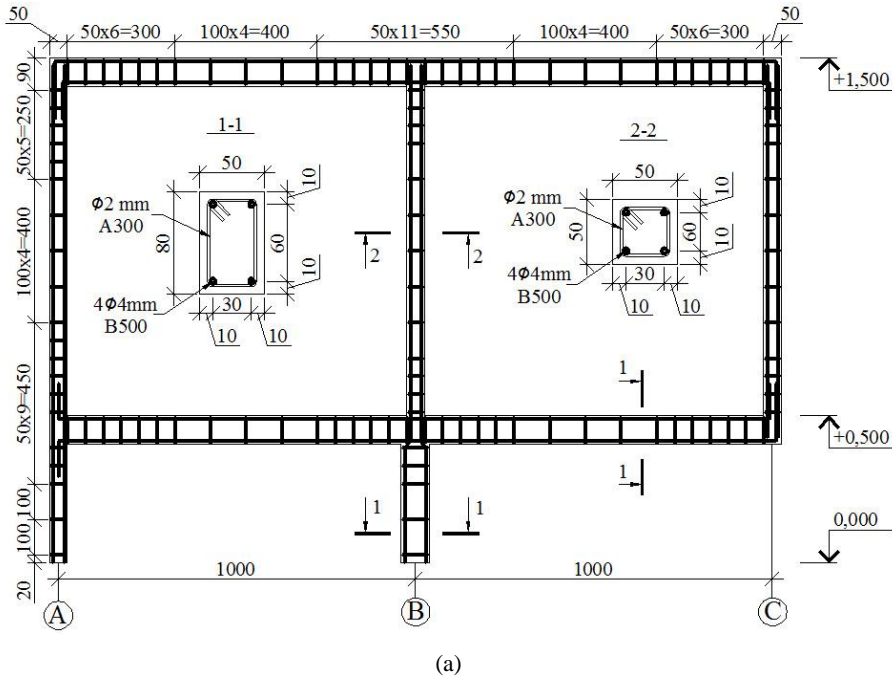


Fig. 4. 2D scale model of RC moment frame investigated by Savin, Kolchunov and Korenkov (2020). (a) Reinforcement scheme; (b) General view of the frame (mirrored to the reinforcement scheme).

The accidental impact caused by the sudden column removal scenario was physically modeled using a special device proposed by Klyueva N.V. and Korenkov P.A. (2018). The device consists of a three-pivot rack and rigid support connected by an additional tie (bar with thread) as presented in Fig. 5 a. The tie (switch off member) ensures the geometric invariability of the device at the stage of loading with an operating load. When simulating the sudden column removal scenario, the additional tie of the device was unscrewed. As a result, the three-pivot rack turned into an instantly changeable system, which is equivalent to the instant removal of the support. The restrain conditions for the bottom nodes of the frame columns can be considered as a hinge with limited linear displacements along the X, Y, Z axes. The device for accidental impact modeling prevents the vertical displacement of the "beam-column" joint. Also, the upper frame nodes were fastened against displacement out of the plane of the structure.

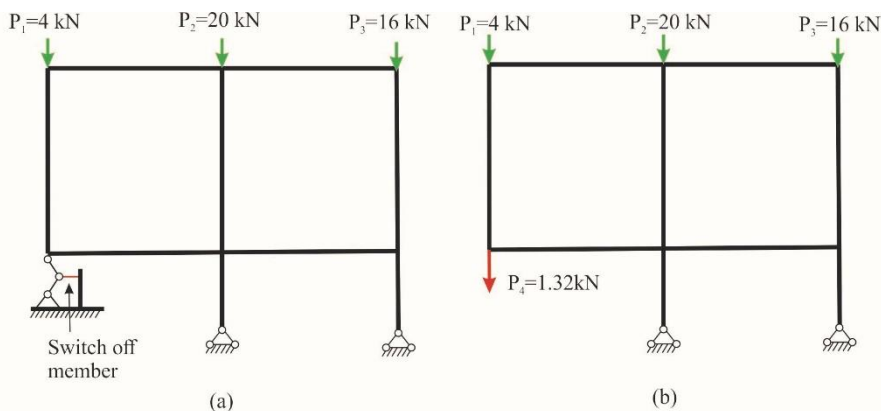


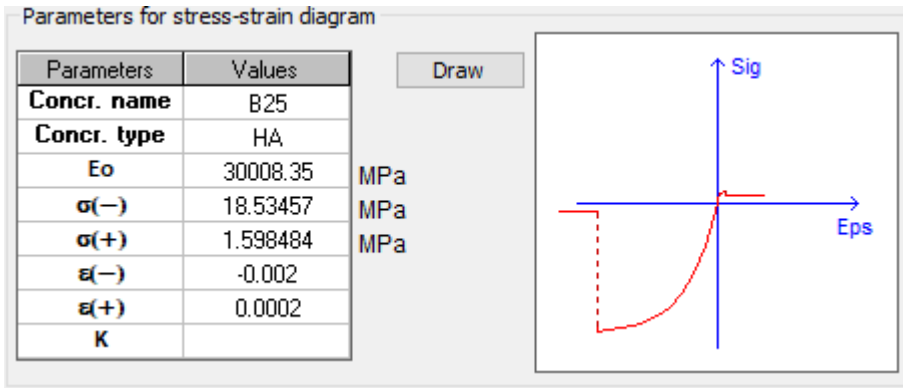
Fig. 5. Calculation scheme of the experimental scale model of the RC frame. (a) Primary calculation scheme; (b) Secondary calculation scheme.

3.2 Finite element model for the test RC frame and simulation of loads and actions

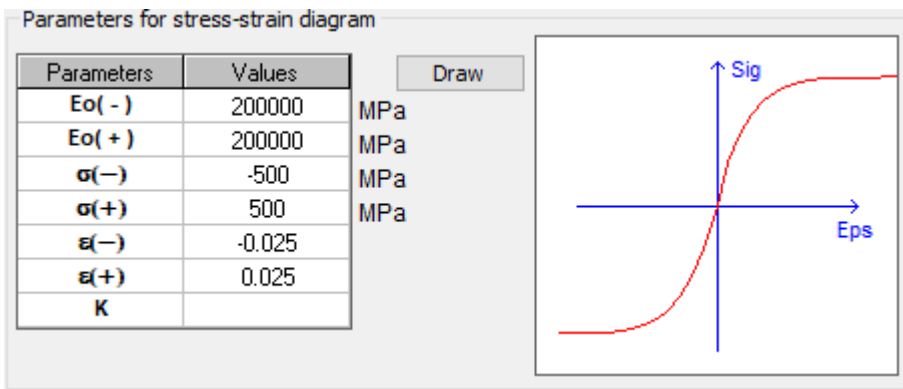
For the purpose of numerical simulation of the test, reinforced concrete frame structural behavior, the Lira-CAD software was applied. This software allows the finite element analysis of building structures. The functions and capabilities of the LIRA-CAD software, theoretical provisions, and design prerequisites are presented in the manual by Gorodetskiy A. et al. (2019).

The columns and beams of the reinforced concrete frame were modeled by physically nonlinear 2D frame bar elements (FE type 202). The relationship between stress and strain was approximated by an exponential law for concrete and reinforcing steel. The general view of the strain-stress curves for the materials are shown in Figures 6a and 6b for concrete and steel respectively. Transverse reinforcement (stirrups) was not considered in the bar FE model. The frame model was restrained against displacement along X, Z at the bottom column nodes at the first floor, and against vertical displacement under the beam-to-column joint placed on the design axis 'C' as it is shown in Figure 5a.

For comparison purposes, a shell-bar FE model was also created, in which the beam-to-column joint of a reinforced concrete frame was modeled using a physically nonlinear rectangular FE of a 2D problem for wall-beam structures (FE type 221). The size of the finite elements of type 221 was taken equal to 1 cm. This is identical to the size of the mesh step of the finite difference method presented in Figure 2a.



(a)



(b)

Fig. 6. Stress-strain diagrams and their main parameters (a) for concrete; (b) for reinforcing steel.

The frame structural behavior under sudden support removal was modeled by a static method based on the approach proposed by Geniev G.A. (1999). Following this approach, the forces acting in the support or structural member at the stage of normal operation should be replaced with a force of the same absolute value but opposite direction in a new design scheme after sudden structural transformation. In the original formulation, the approach proposed by Geniyev G.A., the was carried out for linearly deformable systems. Therefore, when calculating reinforced concrete structures that allow the development of plastic deformations in the members, Almazov V.O., Plotnikov A.I. and Rastorguev B.S. (2011) proposed the use of the dynamic amplification factor k_d , which can be determined by the formula (11):

$$k_d = \frac{k_{pl}}{k_{pl} - 0.5}, \quad (11)$$

where k_{pl} is plasticity factor determined as a full strain to elastic one ratio.

In relation with the formula (11) and the approach proposed by Geniyev G.A. (1999), the force P4 applied to the "beam-column" node to simulate the dynamic effect of the force flows redistribution along alternative load paths can be calculated by the formula (12):

$$P_4 = k_d \cdot N_4 - N_4, \quad (12)$$

where N_4 is a vertical reaction or axial force in the suddenly removed support (member) that acts before accidental impact.

Almazov V.O., Plotnikov A.I., and Rastorguev B.S. noted that dynamic amplification factor (DAF) for reinforced concrete frames takes values in the range from 1.15 to 1.33. In this paper, DAF was taken equal to 1.33 as for the upper boundary of the range.

3.3 Numerical analysis of the 2D stressed RC joint structural behavior according to the proposed method and FEA

Using the relations obtained in Sec. 2.3, we calculated the deformed state of the 2D stressed frame beam-to-column joint placed between the first and the second floors at the "A" axis of the reinforced concrete frame. The calculation results for structural analysis of the 2D beam-column joint exposed to the accidental impact are presented in figure 7, where (a) shows a general view of the considered joint after accidental impact, (b), (c), (d) demonstrate stress contour plot for σ_x , σ_y and τ_{xy} .

For comparison purposes, FE analysis of this 2D stressed joint was performed in Lira-CAD software too. Stress contour plots for σ_x , σ_y and τ_{xy} as well as equivalent stresses N_e calculated as the left part of the inequality (1) presented in figure 8 (a), (b), (c), (d) respectively.

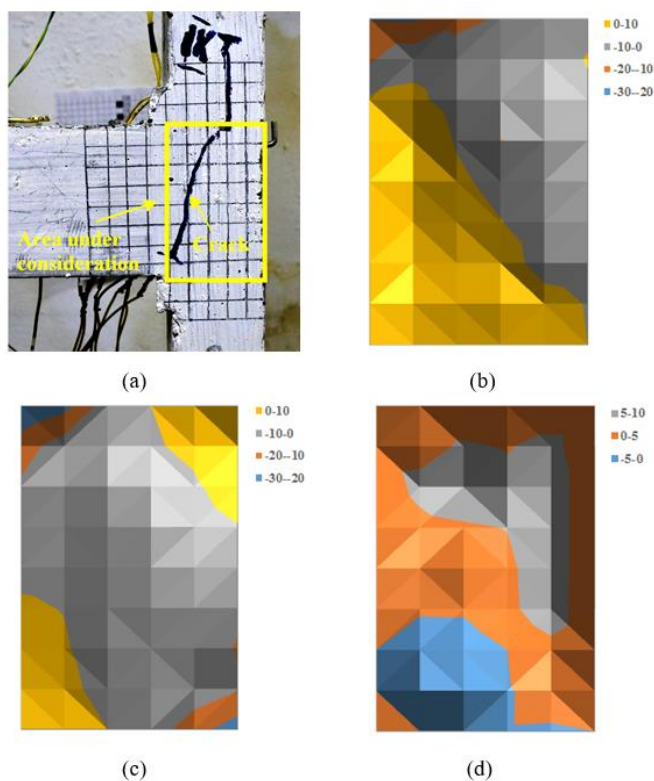


Fig. 7. ‘Beam-column’ joint under consideration and its numerical analysis results by proposed method. (a) View of the beam-to-column joint. The area under consideration highlighted yellow rectangle; (b) Stress contour plot for σ_x , MPa; (c) Stress contour plot for σ_y , MPa; (d) Stress contour plot for τ_{xy} , MPa.

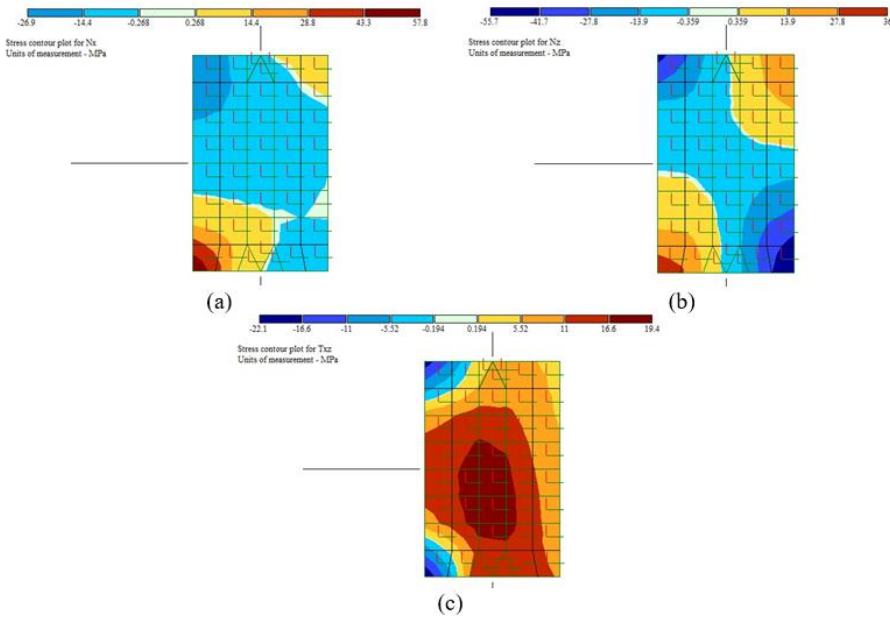


Fig. 8. FEA results for the ‘beam-column’ joint. (a) Stress contour plot for σ_x , MPa; (b) Stress contour plot for σ_y , MPa; (c) Stress contour plot for τ_{xy} , MPa.

In addition, P–delta analysis of the considered frame was performed for the operational and accidental loads. Thus, Fig. 9 presents relations axial force vs. horizontal displacement for loading points in upper nodes of the reinforced concrete frame. And Fig. 10 shows force diagrams (axial force, bending moment, and shear force) for the operational stage and the accidental impact.

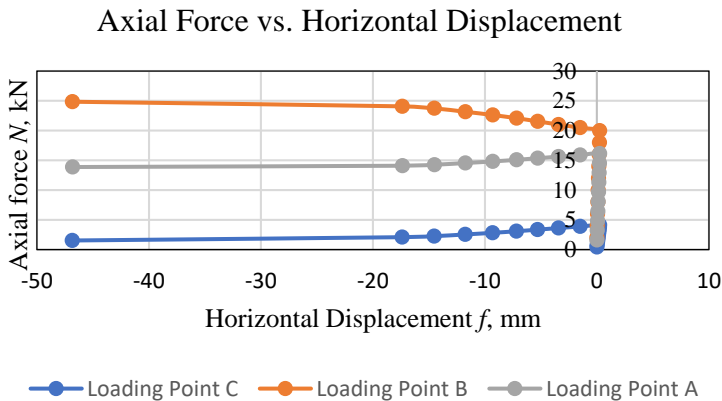


Fig. 9. Axial Force vs. Horizontal Displacement for Loading Points in Upper Nodes of the Reinforced Concrete Frame.

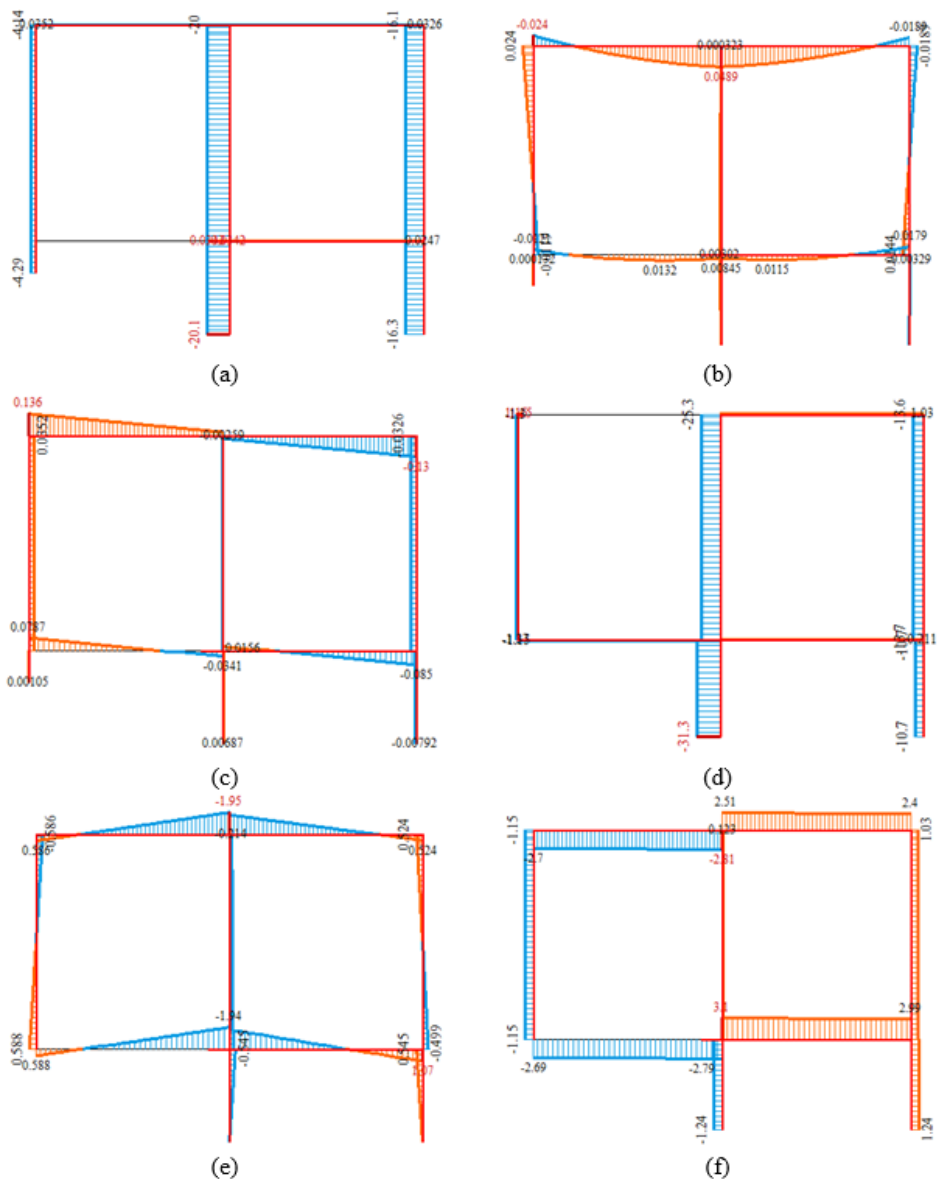


Fig. 10. Force diagrams in bar FE: (a) Axial forces N , kN for primary calculation scheme; (b) Bending moment M , kNm for primary calculation scheme; (c) Shear force V , kN for primary calculation scheme; (d) Axial forces N , kN after structural transformation; (e) Bending moment M , kNm after structural transformation; (f) Shear force V , kN after structural transformation.

4. Discussion

Comparison of stress contour plots obtained with the proposed method and the standard procedure of finite element analysis in the Lira-CAD software shows the following. The distribution of stress contours for σ_x , σ_y and τ_{xy} according to the proposed method and FEM have

some quantitative differences. Such differences are most noticeable in the connection zone where bars connect with a 2D element. The observed effect is expressed as a gradient increase of stresses in the corners of the joint FEM. This can be explained by the significant influence of perfectly rigid bodies. However, in qualitative terms, the stress contour plots obtained by the two methods are nevertheless similar and in the middle of the investigated 2D area have comparable numerical values. In this area, a relatively high level of shear stresses is observed for both methods. That leads to the shear failure of the 2D stressed joint. The calculation results according to the proposed method indicate the destruction of the node through the inclined cross-section in relation to the criterion (1). This is confirmed by the general view of the test model joint: in the middle part of the investigated area, a crack that extends beyond the boundaries of the area has formed.

The calculation results for the bar model presented in Sec. 3.3 shows the change in the direction of bending moments in the structural elements of the frame for both cases: before and after accidental impact. That is shown in Figures 10 (b), (e). There is also a significant increase in shear forces in the beam and columns, as evidenced by Figures 10 (c), (f). The diagrams of axial forces show that the central column of the second floor is additionally loaded by 26.5%, and the conner column along the 'A' axis is unloaded by 15.5%. However, this effect, together with an increase in the shear force and bending moment in the column, is rather negative for a reinforced concrete frame.

P-delta finite element analysis provided in the Sec. 3.3 indicates almost simultaneous buckling of three frame columns under accidental impact. However, such a result was not observed during the tests of a reinforced concrete frame, destruction which was characterized by the formation of cracks in the girders and the failure of the central column only. After that, the dynamic effect quickly decays. These results of the finite element analysis confirm its limited capabilities for the post-critical structural behavior simulation previously noted by Tagel-Din H and Meguro K (2000). Besides, the nonlinear model of reinforcing steel adopted in Section 3.2 did not take into account the hardening of the steel and the possibility of the stress reaching its ultimate values.

5. Conclusions

Summarizing the results of the research carried out, we can conclude the following:

1. The paper proposes a computational model for evaluation of the force resistance of plane-stressed beam-column joint of the monolithic reinforced concrete frame under accidental impact. A distinctive feature of this model is the ability to take into account the discrete reinforcement, as well as an incomplete adhesion of the reinforcement to concrete along the contact surface.
2. As a criterion for assessing the strength of the beam-column joint, it was proposed to use the condition of concrete strength for the plane stress state suggested by Geniyev, Kisyuk and Tyupin.
3. To implement the proposed model, an algorithm for calculating the stress-strain state of the 2D stressed beam-column joint has been developed, which makes it possible to control the convergence of the results.
4. An example of calculating an experimental frame unit based on the proposed approach is considered.

References

- Alanani M, Ehab M, Salem H (2020). Progressive collapse assessment of precast prestressed reinforced concrete beams using applied element method. *Case Stud. Constr. Mater.*, 13, e00457. <https://doi.org/10.1016/j.cscm.2020.e00457>
- Almazov V O, Plotnikov A I, Rastorguev B S (2011) Problems of building resistance to progressive collapse. *Vestnik MGSU*, 2-1, 16-20
- Ahmadi R, Rashidian O, Abbasnia R, Mohajeri Nav F, Usefi N (2016). Experimental and Numerical Evaluation of Progressive Collapse Behavior in Scaled RC Beam-Column Subassembly. *Shock Vib.*, 1–17. <http://www.hindawi.com/journals/sv/2016/3748435/>
- Building Code of Russian Federation SP 63.13330.2018 (2019) Concrete and reinforced concrete structures. General provisions. <https://docs.cntd.ru/document/554403082>
- EN 1992-1-1 (2004) (English): Eurocode 2: Design of concrete structures - Part 1-1: General rules and rules for buildings. <https://www.phd.eng.br/wp-content/uploads/2015/12/en.1992.1.1.2004.pdf>
- Fedorova N, Vu N T (2019). Deformation and failure of monolithic reinforced concrete frames under special actions. *J. Phys. Conf. Ser.* 1425, 012033. <https://iopscience.iop.org/article/10.1088/1742-6596/1425/1/012033>
- Fedorova N, Vu N T, Yakovenko I (2020). Strength criterion for plane stress reinforced concrete element under a special action. *Vestn. MGSU.*, 11, 1513–1522. <http://vestnikmgsu.ru/component/sjarchive/issue/article.display/2020/11/1513-1522>
- Feng D-C, Wu G, Lu Y (2018). Numerical Investigation on the Progressive Collapse Behavior of Precast Reinforced Concrete Frame Subassemblies. *J. Perform. Constr. Facil.*, 32, 04018027. <http://ascelibrary.org/doi/10.1061/%28ASCE%29CF.1943-5509.0001179>
- Feng D-C, Xie S-C, Ning C-L, L, S-X (2019). Investigation of Modeling Strategies for Progressive Collapse Analysis of RC Frame Structures. *J. Perform. Constr. Facil.*, 33, 04019063. <http://ascelibrary.org/doi/10.1061/%28ASCE%29CF.1943-5509.0001328>
- Geniyev G, Kisyuk V, Tyupin G (1974). Plasticity theory of concrete and reinforced concrete. Stroyizdat, Moscow, USSR.
- Geniyev G.A. (1999) On Dynamic effects in bar structural systems made of physically nonlinear fragile materials. *Promyshlennoye i grazhdanskoye Stroitel'stvo*, 9, 23–24.
- Gorodetskiy A, Strelets-Streletskiy E, Zhuravlev V, and Vodop'yanov R (2019) Lira-CAD. Chapter I. Basics. Publishing LIRALAND, 154 p. https://www.liraland.ru/public_private/lira/2019/book_lirasapr_the_basics_2019.pdf
- Gudmundsson G, Izzuddin B (2008). The “sudden column loss” idealisation for disproportionate collapse assessment. *Struct. Eng.*, 88(6), 22-26.
- Hayati N, Hamid A (2015). Seismic Performance of Interior Beam-Column Joint With Fuse-Bar Designed Using Ec8 Under In-Plane Lateral Cyclic Loading. *Proc. International Conference on Disaster Management and Civil Engineering (ICDMCE'15)* Oct. 1-3, 2015, Phuket, Thailand. <http://ur.st.org/siteadmin/upload/3277U1015302.pdf>
- Hwang S, Lee H (2000). Analytical Model for Predicting Shear Strengths of Interior Reinforced Concrete Beam-Column Joints for Seismic Resistance. *ACI Struct. J.* 97, 35–44. <http://www.concrete.org/Publications/ACIMaterialsJournal/ACIJJournalSearch.aspx?m=details&ID=831>
- Izzuddin B, Vlassis A, Elghazouli A, Nethercot D (2008). Progressive collapse of multi-storey buildings due to sudden column loss - Part I: Simplified assessment framework. *Eng. Struct.*, 30, 1308-1318. <https://doi.org/10.1016/j.engstruct.2007.07.011>
- Kai Q, Li B (2012). Dynamic performance of RC beam-column substructures under the scenario of the loss of a corner column-Experimental results. *Eng. Struct.*, 42, 154-167. [10.1016/j.engstruct.2012.04.016](https://doi.org/10.1016/j.engstruct.2012.04.016)

- Klyueva N V, Korenkov P A (2018) A device for the experimental determination of dynamic loading in frame-rod structural systems. Patent of Russia No. 2642542
- Kolchunov V, Savin S (2018). Survivability criteria for reinforced concrete frame at loss of stability. *Mag. Civ. Eng.*, 80, 73–80. <https://engstroy.spbstu.ru/en/article/2018.80.7/>
- Kolchunov V, Fedorova N, Savin S, Kovalev V, Iliushchenko T (2019). Failure simulation of a RC multi-storey building frame with prestressed girders. *Mag. Civ. Eng.* 92, 155–162. [https://engstroy.spbstu.ru/userfiles/files/2019/8\(92\)/13.pdf](https://engstroy.spbstu.ru/userfiles/files/2019/8(92)/13.pdf)
- Li Y., Lu X., Guan H., Ren P. (2016). Numerical investigation of progressive collapse resistance of reinforced concrete frames subject to column removals from different stories *Adv. Struct. Eng.*, 19, 314–326. <http://journals.sagepub.com/doi/10.1177/1369433215624515>
- Marjanishvili S, Agnew E (2006). Comparison of Various Procedures for Progressive Collapse Analysis. *J. Perform. Constr. Facil.* 20, 4, 365–374. [https://doi.org/10.1061/\(ASCE\)0887-3828\(2006\)20:4\(365\)](https://doi.org/10.1061/(ASCE)0887-3828(2006)20:4(365))
- Sasani M, Werner A, Kazemi A (2011). Bar fracture modeling in progressive collapse analysis of reinforced concrete structures. *Eng. Struct.*, 33, 401–409. <http://dx.doi.org/10.1016/j.engstruct.2010.10.023>
- Savin S, Kolchunov V, Korenkov P (2020). Experimental research methodology for the deformation of RC frame under instantaneous loss of column. *IOP Conf. Ser. Mater. Sci. Eng.*, 962, 022054. <https://doi.org/10.1088/1757-899X/962/2/022054>.
- Shan L, Petrone F, Kunnath S (2019). Robustness of RC buildings to progressive collapse: Influence of building height. *Eng. Struct.*, 183, 690–701. <https://doi.org/10.1016/j.engstruct.2019.01.052>
- Tagel-Din H, Meguro K (2000). Nonlinear simulation of RC structures using applied element method. *Struct. Eng. Eng.* 17, 137–148. https://www.jstage.jst.go.jp/article/jscej1984/2000/654/2000_654_13/_article/-char/ja/
- Tsonos A.G. Effectiveness of CFRP-jackets and RC-jackets in post-earthquake and pre-earthquake retrofitting of beam–column subassemblages. *Eng. Struct.*, 30, 777–793. <https://doi.org/10.1016/j.engstruct.2007.05.008>
- Wang H, Zhang A, Li Y, Yan W (2014). A Review on Progressive Collapse of Building Structures. *Open Civ. Eng. J.*, 8, 183–192.
- Yu J, Tan K (2013). Structural Behavior of RC Beam-Column Subassemblages under a Middle Column Removal Scenario. *J. Struct. Eng.*, 139, 233–250. <http://ascelibrary.org/doi/10.1061/%28ASCE%29ST.1943-541X.0000658>
- Yu J, Luo L, Li Y (2018). Numerical study of progressive collapse resistance of RC beam-slab substructures under perimeter column removal scenarios. *Eng. Struct.*, 159, 14–27. <https://doi.org/10.1016/j.engstruct.2017.12.038>